Contribution from the Anorganisch-chemisches Institut and Lehrstuhl für Theoretische Chemie, Technische Universität München, D-8046 Garching, Federal Republic of Germany

Electronic Structure of $[(\eta^5\text{-}C_5Me_5)_3Re_3(\mu\text{-}O)_6]^{2+}$ and of Related Early-Transition-Metal Arene Clusters

Peter Hofmann,*† Notker Rösch,*‡ and Helmut R. Schmidt†

Received August 1, 1986

The electronic structure of the recently synthesized trimetal cluster ion $[(\eta^5\text{-}C_5Me_5)_3Re_3(\mu\text{-}O)_6]^{2+}$ has been studied (by using its Cp model) theoretically with both the extended Hückel and the SCF Xα–SW method. Both independent computational schemes agree in their bonding description of the highly symmetric cluster ion (pseudo-D_{3h} symmetry), yielding four lowest lying metal-derived levels belonging to the symmetries $1a_1'$, $1e'$, $2a_1'$, and $2e'$. These MOs are filled with four valence electrons in the case of the Re_3 cluster ion, resulting in a triplet ground state, at variance with the reported interpretation of NMR data, which indicate diamagnetism. The same MO sequence is found by EH calculations and is used to rationalize the electronic structure of the related early-transition-metal clusters of the general type $[(\eta^6\text{-}C_6Me_6)_3M_3(\mu\text{-}X)_6]^{n+}$ (M = Nb, Ta, Ti, Zr; X = Cl, Br; n = 1, 2; C_6Me_6 = hexamethylbenzene). The occupation pattern of the four relevant levels in all these clusters varies between five and eight electrons and correlates well with the available information on structure, bonding, and electrochemical behavior of these compounds.

Recently the synthesis of the fascinating new trinuclear Re cluster system $[(\eta^5\text{-}C_5Me_5)_3Re_3(\mu\text{-}O)_6](ReO_4)_2$ has been reported by Herrmann and co-workers.[1] A single-crystal X-ray diffraction study[1] revealed the presence of the highly symmetric cluster cation **1**, in this perrhenate salt.

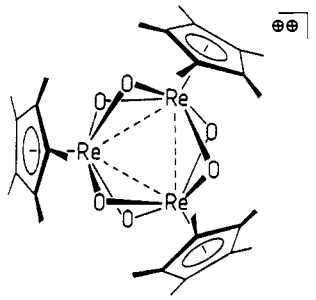

1

The Re_3O_6 core of **1** consists of a trigonal prism of six oxygens, the three rhenium atoms cap the three rectangular faces, and each rhenium is coordinated by an $\eta^5\text{-}C_5Me_5$ ligand. Alternatively, **1** can be viewed as an equilateral Re_3 triangle with six bridging μ-oxygens and a terminal $\eta^5\text{-}C_5Me_5$ group attached to each metal center. So **1** is another member of the large class of trinuclear clusters of early transition metals, which have found much experimental[2] and theoretical[3] attention during the recent past. Two terminological schemes have been used in the literature to classify such trinuclear clusters: according to Müller et al.,[2] **1** belongs to their category A (no capping μ_3-type ligands); in the terminology of Jiang et al.,[3] **1** is of the U_6 type (uncapped, six bridging μ_2 ligands) and has the general composition $M_3Y_6Z_3$ (M = Re, Y = μ-O, Z = $\eta^5\text{-}C_5Me_5$; formally, the latter is electronically equivalent to three terminal two-electron ligands).

A number of points associated with experimental observations for **1** and with simple theoretical considerations and questions raised our interest and formed the impetus for the study to be described here.[4] Let us outline these points first.

Most importantly, we were intrigued by the fact that **1** has been reported to be diamagnetic.[1] Simple electron counting apparently is insufficient to predict either that or to deduce the presence of unpaired electrons for the electronic ground state of **1**. The three metal atoms are left with a total of four valence electrons, resulting in a formal oxidation state of $5^2/_3$ per Re, and in a formal Re–Re bond order of $^2/_3$.

There are, however, simple qualitative electronic structure considerations, which seem to contradict a singlet ground state of **1**. The argument goes as follows. In a rather formal sense, each Re can be visualized as the central atom of a local "four-legged piano-stool" complex Cp^*ML_4, as shown in **2**, with L being

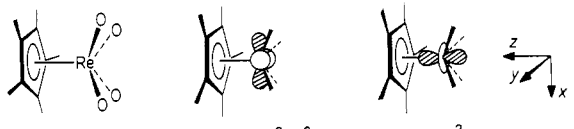

2 **3** (x^2-y^2) **4** (z^2)

oxygen atoms ($Cp^* = \eta^5\text{-}C_5Me_5$). The electronic structure and MO level sequence of such systems are well-known.[5] Only two of the metal d levels appear at low energy; within the coordinate system shown above these are $x^2 - y^2$ (**3**), and z^2 (**4**).

The other 3 orbitals of d type, xz, yz, and xy, are destabilized more strongly by metal–ligand interactions. If we take, for the sake of simplicity in this qualitative picture, the $\eta^5\text{-}C_5Me_5$ ligands as effectively rotationally symmetric, then the regular molecular geometry of **1** with formally three piano-stool fragments will lead to symmetry-adapted ("D_{3h}") linear combinations of fragment orbitals **3** and **4**. Six cluster levels will result, namely two of a_1' symmetry and two of e' symmetry for both the $x^2 - y^2$ and the z^2 set. Obviously, due to their identical symmetry, these two z^2-based and $x^2 - y^2$-based sets will mix with each other, leading to a low energy $a_1' + e'$ triad of MOs and pushing the other $a_1' + e'$ set up. It is easy to conclude from the topology and from overlap criteria for mutually interacting fragment orbitals **3** and **4**, that the resulting MO pattern for **1** should resemble the picture shown in Figure 1. In passing we note that the same level sequence, with the second symmetric level $2a_1'$ above $1e'$, applies also in the case of a "naked" M_3 triangle, as has been shown elsewhere.[3]

The low-lying orbitals $1a_1'$ and $1e'$ will display predominantly z^2 character at the metal centers, with some admixture of $x^2 - y^2$, the quantitative extent of which cannot a priori be determined of course. Qualitative sketches of the two nondegenerate levels $1a_1'$ and $2a_1'$ and of both e' orbitals (only the antisymmetric component is shown) are included in Figure 1. $1a_1'$ and its de-

† Anorganisch-chemisches Institut.
‡ Lehrstuhl für Theoretische Chemie.

(1) (a) Herrmann, W. A.; Serrano, R.; Ziegler, M. L.; Pfisterer, H.; Nuber, B. *Angew. Chem.* **1985**, *97*, 50–51; *Angew. Chem. Int. Ed. Engl.* **1985**, *24*, 50–51. (b) Herrmann, W. A.; Serrano, R.; Küsthardt, U.; Guggolz, E.; Nuber, B.; Ziegler, M. L. *J. Organomet. Chem.* **1985**, *287*, 329–344. (c) Herrmann, W. A. *J. Organomet. Chem.* **1986**, *300*, 111–138.
(2) A review can be found in: Müller, A.; Jostes, R.; Cotton, F. A. *Angew. Chem.* **1980**, *91*, 921–929; *Angew. Chem., Int. Ed. Engl.* **1980**, *19*, 875–882. A second extensive listing of experimental work, synthetic and structural, has been given in ref 3.
(3) Jiang, Y.; Tang, A.; Hoffmann, R.; Jinling, H.; Lu, J. *Organometallics* **1985**, *4*, 27–34 and references therein. See also the section on electronic structures in ref 2.
(4) For a preliminary account of this work see: Hofmann, P.; Rösch, N. *J. Chem. Soc., Chem. Commun.* **1986**, 843.
(5) Kubacek, P.; Hoffmann, R.; Havlas, Z. *Organometallics* **1982**, *1*, 180–188.

0020-1669/86/1325-44 0$01.50/0

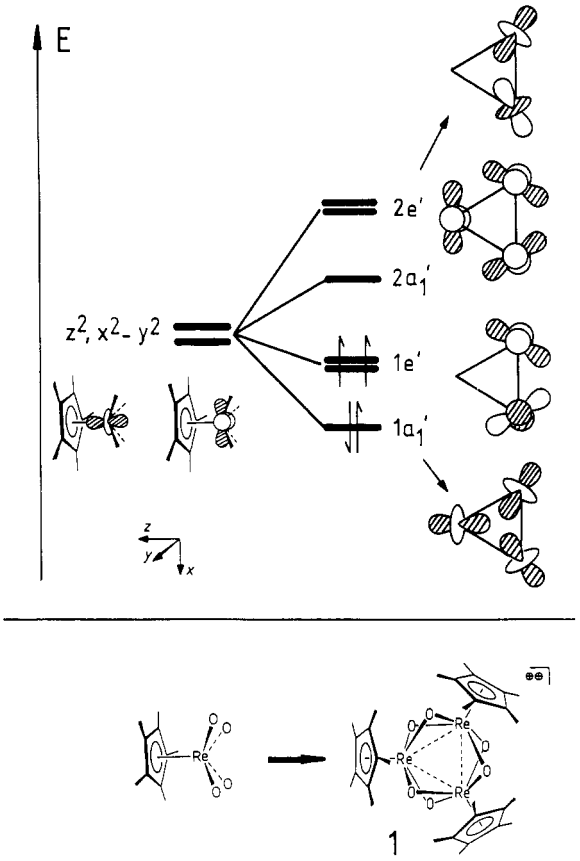

Figure 1. Qualitative level scheme of **1** as derived from the electronic structure of three formal "four-legged piano-stool" fragments "$(C_5Me_5)ReO_4$", labeled according to pseudo-D_{3h} symmetry.

generate counterpart 1e' evidently are the delocalized equivalents of three metal–metal bonds. Consequently a purely symmetry-based and qualitative reasoning would predict the presence of two unpaired electrons in **1** for its electron count of 4. A singlet ground state, on the other hand, should then be coupled to a more or less noticeable Jahn–Teller distortion of the trinuclear cluster system.

At this point it is also appropriate to recall the existence and properties of a series of other trinuclear clusters of precisely the same structural type and stoichiometry as found for **1**. Fischer and Röhrscheid[6a] 20 years ago prepared the cations **5** and **7**; also known is compound **8**.[7] The Nb/Cl system has been structurally

$[(\eta^6\text{-}C_6Me_6)_3Nb_3(\mu\text{-}Cl)_6]^+$ (**5**)

$[(\eta^6\text{-}C_6Me_6)_3Nb_3(\mu\text{-}Cl)_6]^{2+}$ (**6**)

$[(\eta^6\text{-}C_6Me_6)_3Ta_3(\mu\text{-}Cl)_6]^+$ (**7**)

$[(\eta^6\text{-}C_6Me_6)_3Nb_3(\mu\text{-}Br)_6]^+$ (**8**)

$[(\eta^6\text{-}C_6Me_6)_3M_3(\mu\text{-}Cl)_6]^+$ (**9**)

M = Ti, Zr

investigated.[8] A total of eight metal electrons are counted here; the systems are diamagnetic. The oxidized paramagnetic species **6** with only seven electrons has been found to remain practically unaffected structurally upon oxidation, compared to its diamagnetic eight-electron precursor.[9] Also known are analogous Ti and Zr compounds **9**:[6a] they hold one electron less than **1**, and a magnetism due to one unpaired electron is found experimentally, but no structure determination for any of them has been reported yet. The symmetry-based qualitative picture of Figure 1 ought to hold for these clusters as well. So apparently the expectation of a triplet ground state for the Re cluster ion **1** seems to be mandatory, unless a Jahn–Teller distortion creates a singlet. Recall, however, that the experimental structure of **1**[1] displays perfect threefold symmetry.

There is a number of rather severe caveats nonetheless, which eventually have led us to the detailed computational study to be described below. Although the above reasoning follows the lines that have proven to be qualitatively reliable for related trinuclear metal clusters in the work of Cotton et al.[2] and Hoffmann et al.[3] (in which the structural type of **1** has not been discussed), the actual role of coordinated "electropositive" arene ligands of the cyclopentadienyl or benzene type is somewhat difficult to assess from qualitative arguments. Such ligands, although only "terminal",[10] might possibly lead to level inversions compared to the levels shown in Figure 1. Note that a pattern of $2a_1'$ below 1e' would invalidate the prediction of a triplet. In fact, $2a_1'$ at the metals has δ symmetry toward the faces of the arene ligands, thus offering a chance to get $2a_1'$ pushed down, possibly even below 1e', by back-bonding to empty arene π^* levels. Furthermore, **1** is the only available example of a U_6 system with exclusively μ-O ligands. Metal–oxygen covalency might have an important influence.

Given the discrepancy between the reported diamagnetism and the qualitative expectation of two unpaired electrons on one hand and taking into account the incertainties of qualitative arguments (although mainly symmetry based) for **1** on the other side, it seemed worthwhile to study the electronic structure of **1** in more detail.

Two independent methodologies have been employed: extended Hückel MO calculations,[11] the results of which will be described first, leading to a conceptionally transparent one-electron level picture of **1**; second, electronic structure calculations within the local density formalism, utilizing the SCF $X\alpha$–SW approach,[12] which should yield results of higher quantitative reliability. Computational and geometric details, as far as they are not apparent from the text, are collected within the Appendix.

For the sake of comparison we will also include in our discussion the results of EH calculations for systems like **5**. This should allow conclusions with respect to metal–metal bonding, should help to clarify the role of the bridging μ_2 ligands, and should allow judgment of the generality of the derived level schemes.

In order to reduce the explicit calculations to an easier tractable size within both methods, the arene ligands C_5Me_5 and C_6Me_6 have been replaced in all cases by C_5H_5 and C_6H_6. The basic results should be unaffected by this simplification.

The $Re_3O_6^{5+}$ Core

As stated above, we cannot a priori expect the terminal arene groups, i.e. C_5Me_5 in **1**, to be innocent with respect to the final level ordering of **1**. As a consequence, different from the above "piano-stool-based" picture, we will describe the electronic structure of the electron-deficient cluster cation **1** in terms of a $Re_3O_6^{5+}$ core, interacting in the final step of assembling the complete system with three terminal C_5Me_5 anions, replaced by C_5H_5 in our model of **1**, $[(\eta^5\text{-}C_5H_5)_3Re_3(\mu\text{-}O)_6]^{2+}$.

The metal-based levels of a $Re_3O_6^{5+}$ fragment, D_{3h}, as they emerge from an extended Hückel calculation are easily understood.

(6) (a) Fischer, E. O.; Röhrscheid, F. *J. Organomet. Chem.* **1966**, *6*, 53–66. (b) Stollmaier, F.; Thewalt, U. *J. Organomet. Chem.* **1981**, *208*, 327–334.
(7) King, R. B.; Braitsch, D. M.; Kapoor, P. N. *J. Am. Chem. Soc.* **1985**, *97*, 60–64.
(8) (a) Churchill, M. R.; Chang, S. W.-Y. *J. Chem. Soc., Chem. Commun.* **1974**, 248–249. (b) Stollmaier, F.; Thewalt, U. *J. Organomet. Chem.* **1981**, *222*, 227–233.
(9) (a) Goldberg, S. Z.; Spivack, B.; Stanley, G.; Eisenberg, R.; Braitsch, D. M.; Müller, J. S.; Abkowitz, M. *J. Am. Chem. Soc.* **1977**, *99*, 110–117. (b) For recent electrochemical work on **5** and **6** see: Boyd, D. C.; Gebhard, M.; Mann, K. R. *Inorg. Chem.* **1986**, *25*, 119–120.
(10) In ref 3, terminal, electronegative monodentate ligands have been shown to be the least important ones for the cluster level sequence in systems with also μ_2 and μ_3 ligands.
(11) Hoffmann, R. *J. Chem. Phys.* **1963**, *39*, 1397–1412.
(12) (a) Slater, J. C. *The Self-Consistent Field for Molecules and Solids*; McGraw-Hill: New York, 1974. (b) Rösch, N. *NATO ASI Ser., Ser. B* **1977**, *24*, 1–143.

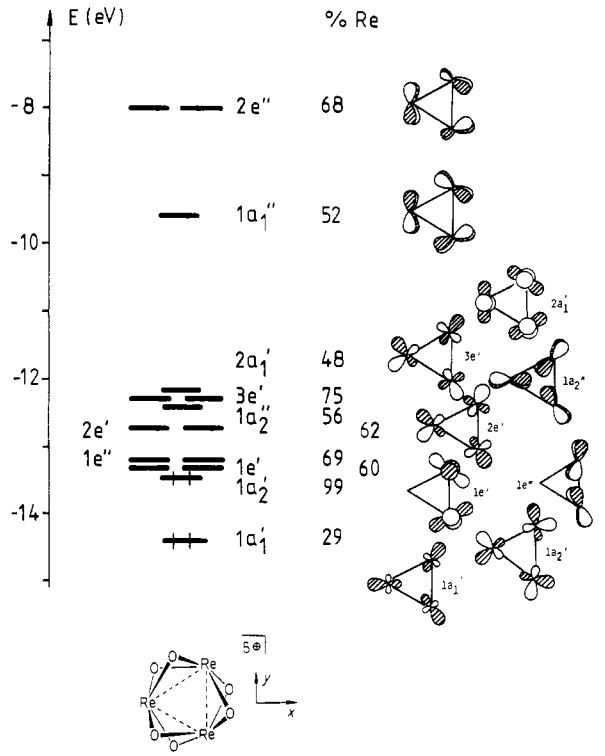

Figure 2. d-Block levels of the D_{3h} $Re_3O_6^{5+}$ core of **1** from an EH calculation. Also given are the symmetry type of each level, its Re_3 contribution to the wave function, and a simplified representation of the metal contributions to the orbitals (only one component of each appropriate e representation shown).

It is convenient, to start out from a Re_3 triangle with a local coordinate system[3] at each center as shown in **10**, with x and z

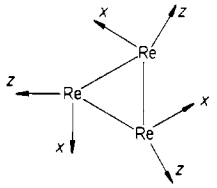

10

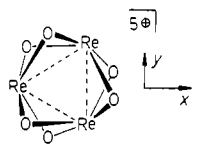

11

axes in the Re_3 plane, the y axes being perpendicular to it. The 15 symmetry-adapted linear combinations resulting from the three sets of five metal d AOs then transform as $a_1' + e'$ (z^2), $a_1' + e'$ ($x^2 - y^2$), $a_1'' + e''$ (xy), $a_2' + e'$ (xz), and $a_2'' + e''$ (yz). In the actual calculation all levels of the same symmetry of course will mix and repel each other, and, a certain level ordering will result,[13] depending upon the nodal and overlap situation in each MO. We do not need to discuss the Re_3 fragment MOs in full detail; instead, we can directly turn to the consequences of interacting the Re_3 fragment with six μ-O bridging ligands, yielding the Re_3O_6 core of interest to us, which has a +5 charge for the electron count of **1** and which is shown in **11**. The effect of the six bridging μ-oxygen ligands will be to destabilize, to a variable degree (as a function of Re–O overlap), the Re_3 d levels. We could again use local coordinate systems, appropriate for each bridging oxygen atom, and derive the symmetry adapted linear combinations of the sixfold set of three 2p levels at the oxygens and could thus construct all MOs of the complete system $Re_3O_6^{5+}$. Instead we directly present the calculated energy levels of the d block in Figure 2. Also given is their symmetry designation and the metal

(13) See a more detailed pictorial representation in the case of Mo_3 in ref 3. For Fenske–Hall calculations on Mo_3O_6 compare also: Bursten, B. E.; Cotton, F. A.; Hall, M. B.; Najjar, R. C. *Inorg. Chem.* **1982**, *21*, 302–307.

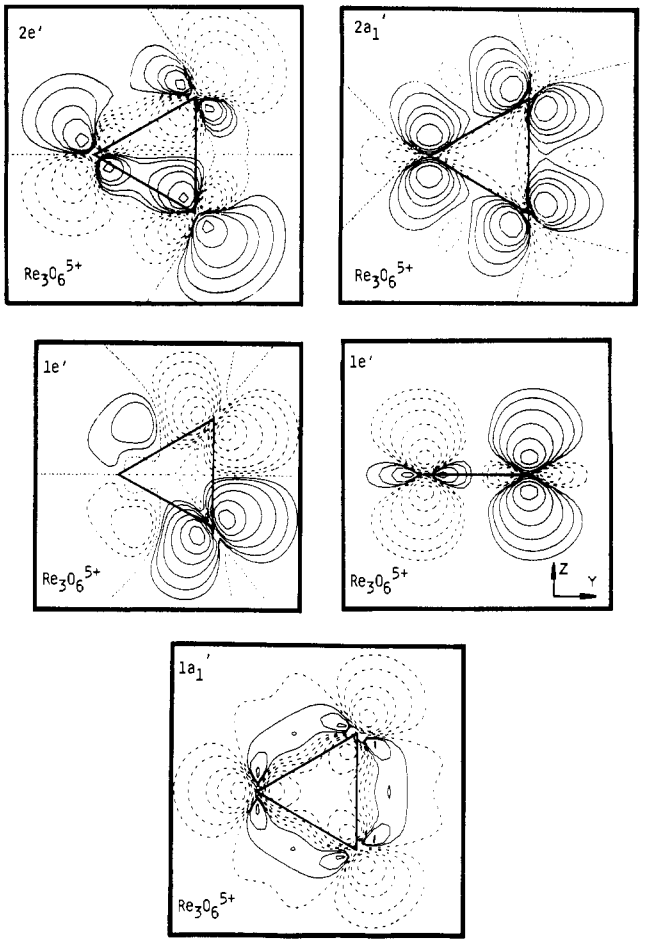

Figure 3. Wave function contour plots (EH) for $Re_3O_6^{5+}$, relevant to the electronic structure of **1**. The MOs $1a_1'$, $2a_1'$, $1e'$, and $2e'$ (the antisymmetric component of it) are plotted within the Re_3 plane; the (antisymmetric) $1e'$ member is also plotted in a plane that is perpendicular to the Re_3 triangle and contains two Re centers. See also Figure 2. Solid lines (broken lines) correspond to positive (negative) sign of the wave function. The contour values are ±0.2, ±0.1, ±0.05 ±0.025, ±0.0125, and ±0.0625. The –·– lines are zero contours.

contribution to the wave function (in % Re) along with a qualitative representation of the metal part of the orbitals (only one component of each e set shown). In some of the $Re_3O_6^{5+}$ orbitals the oxygen contribution approaches 50%. Accordingly their Re–O bonding counterparts at lower energy (not shown in Figure 2) are also rather delocalized and, along with the quite broad energy region over which the 15 levels spread out, reflect some covalent character of the core $Re_3O_6^{5+}$.

In particular the lowest level shown in Figure 2, $1a_1'$, carries much more oxygen than rhenium contributions to the wave function in EH. We will come back to this point later. It is informative to take a look at some of the computed orbitals of $Re_3O_6^{5+}$ as plotted from the wave functions. Figure 3 represents contour diagrams for $1a_1'$, $1e'$, $2a_1'$, and $2e'$ (one e' component only), which will turn out to be the $Re_3O_6^{5+}$ levels of importance for the electronic structure of the complete cluster **1**.

Having delineated the level structure of the $Re_3O_6^{5+}$ core, we are prepared now to assemble $[(\eta^5\text{-}C_5H_5)_3Re_3(\mu\text{-}O)_6]^{2+}$ (written as $Cp_3Re_3O_6^{2+}$ in the following), by taking into account the effect of three $C_5H_5^-$ groups bound in an η^5 fashion to each Re center. The $Re_3O_6^{5+}$ fragment itself in our EH calculations is characterized by a set of five d type levels above $1a_1'$ ($1a_2'$, $1e'$, and $1e''$; see Figure 2), which are very close in energy and hold two electrons, and the essential question is whether the full cluster system will indeed retain this or a similar pattern, indicative of two unpaired electrons. We will in fact see that just one half-filled e set will be left over after the arene ligands have come into the picture, but before we enter this discussion we will now turn to

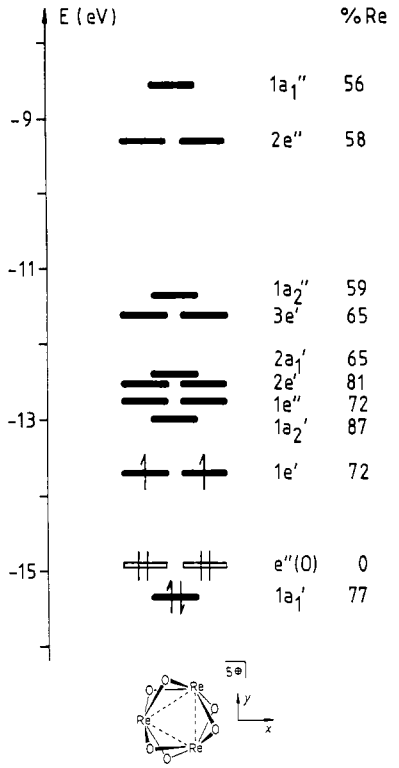

Figure 4. d-Block levels of the D_{3h} $Re_3O_6^{5+}$ core of **1** from an SCF Xα–SW calculation. Also given are the symmetry type of each level and its Re_3 contribution to the orbitals. The same simplified representations of the metal contributions to the wave functions apply as given for the corresponding levels in Figure 2.

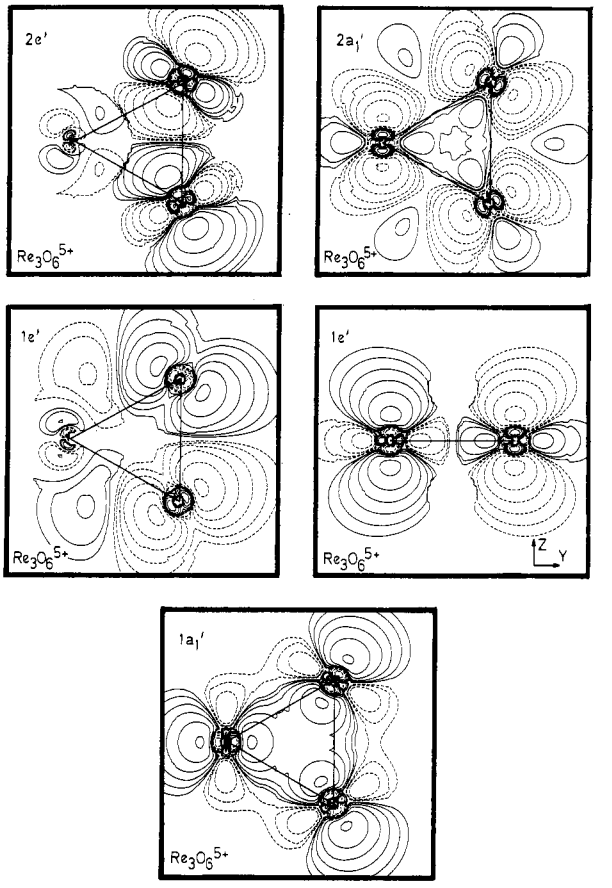

Figure 5. Xα–SW orbital contour plots for the $Re_3O_6^{5+}$ levels relevant to the electronic structure of **1**. The same layout (planes shown, contour values used) has been employed as in the corresponding panels of Figure 3.

the $Re_3O_6^{5+}$ fragment as described by the Xα–SW method.

The d block energy levels of $Re_3O_6^{5+}$, as calculated by this approach, are presented in Figure 4 in the same fashion as in Figure 2, including the metal contribution to the various orbitals (in % Re). The qualitative representations of the metal part of the wave functions are not displayed since they are virtually identical with those given in the EH level diagram. The close similarities between the two diagrams will become apparent after their differences have been discussed.

The overall splitting of the Xα levels is 6.9 eV, about 50% larger than that of the EH levels—a phenomenon well-known from cluster calculations.[14] The $1a_1'$ orbital, an almost pure linear combination of z^2 Re atomic contributions (see Figure 5), is quite strongly metal–metal bonding – much more so than the corresponding EH level. Consequently, it drops even below the top oxygen 2p derived orbital e''(O) at −14.93 eV, which exhibits no localization on the metal atoms. The HOMO of the $Re_3O_6^{5+}$ core is the 1e' level, carrying two of the four metal valence electrons. The $1a_2'$ orbital, the HOMO in the EH calculation, lies about 0.7 eV higher. Thus, the Xα level sequence is already a harbinger of the electronic structure that is to emerge from the inclusion of the cyclopentadienyl ligands. A contour plot representation for the same levels as in Figure 3, now from the Xα calculation, is shown in Figure 5.

The level pattern at medium energy range (1e' to $1a_2''$ for Xα; $1a_2'$ to $2a_1'$ for EH) looks rather different at first sight. However, the pairs of levels generated from one specific set of Re orbitals (z^2, xy, etc.) always appear in the same energy order with the exception of the xz-derived levels $1a_1''$ and 2e''. Please note that the pairing for the pertinent levels of Figure 2 is $1a_1'$ – 2e' and 1e' – $2a_1'$, as may be confirmed from the contour plots of Figures 3 and 5. These sets of orbitals have a stronger localization on the metal cluster in the Xα calculation and consequently appear at relatively lower energies. The yz-derived set $1a_2'$ + 3e' is more Re–O antibonding in the Xα than in the EH calculation, where these orbitals are practically Re–O nonbonding. So they come at relatively higher energies in Xα. This explains the reversal of the HOMO–LUMO levels observed between the two calculations. Let us finally mention that the energetic location of the xz-derived levels $1a_1''$ + 2e'' is consistent with their strong Re–O antibonding character. Their corresponding bonding partners at −19.70 eV (a_1'') and at −18.47 eV (e'') appear in reverse order as is to be expected. Indeed, the a_1'' level is the lowest lying of the bonding-O 2p-derived manifold. This level exhibits a sizable Re contribution of 47% but is just one of several such orbitals leading together to an appreciably large covalent Re–O interaction in the $Re_3O_6^{5+}$ fragment.

To summarize, we may conclude that both computational approaches give a rather similar description of the electronic structure of the $Re_3O_6^{5+}$ core. The main differences lie in highly Re–O antibonding levels, which are insignificant both for the $Re_3O_6^{5+}$ fragment and for its role within the complete cluster ion **1** or in the absolute ordering of rather closely spaced levels. The latter orbitals, however, are those most affected by the cyclopentadienyl ligands as the following discussion will show. Therefore the slightly different starting point will turn out to be quite unimportant after the strong metal–arene interaction has been taken into account.

$Cp_3Re_3O_6^{2+}$

Let us consider now, how the three terminal, η^5-bound $C_5Me_5^-$ ($C_5H_5^-$ in our calculations) ligands affect the level structure of the $Re_3O_6^{5+}$ core. For the sake of simplicity and for easier comparison to the aforementioned hexamethylbenzene clusters **5–9** with true D_{3h} symmetry, we will regard a $C_5H_5^-$ ligand as rotationally invariant around its fivefold axis. $Cp_3Re_3O_6^{2+}$ then is of D_{3h} symmetry as well, and we can use the D_{3h} symmetry labels throughout.[15] Each Cp^- ligand brings along its well-known set

(14) Messmer, R. P.; Knudson, S. K.; Johnson, K. H.; Diamond, J. B.; Yang, C. Y. *Phys. Rev. B* **1976**, *13*, 1396–1415.

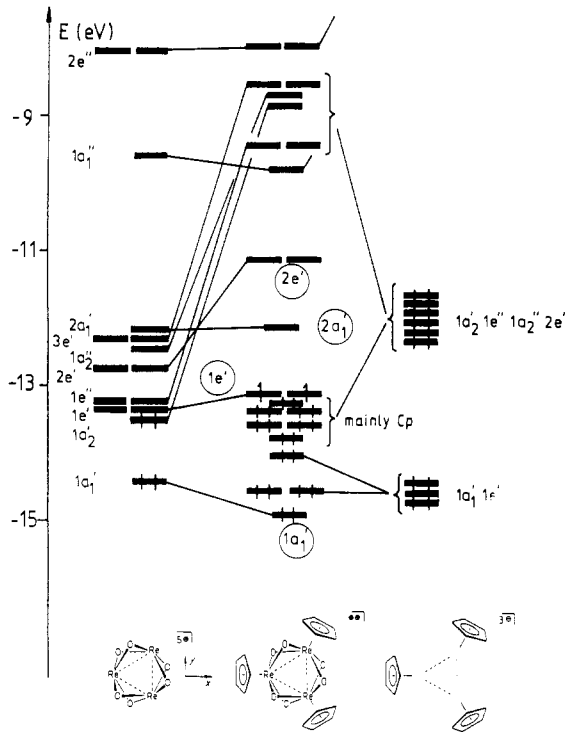

Figure 6. Interaction diagram (EH) between the d-block levels of the $Re_3O_6^{5+}$ core and the MOs of the Cp_3^{3-} ligand system, with pseudo-D_{3h} symmetry. Levels of σ type of the three C_5H_5 ligands, energetically between the two occupied π blocks, practically noninteracting with $Re_3O_6^{5+}$, have been omitted in the diagram.

of five π orbitals with a total of six electrons, their local symmetry towards each η^5-bound metal center is of σ, π, and δ type as shown schematically in **12–14**.

12 (σ) 13 (π) 14 (δ)

A total of 15 symmetry-adapted linear combinations of the five π MOs of the $(Cp_3)^{3-}$ fragment will then interact with the $Re_3O_6^{5+}$ building block. Each $(Cp_3)^{3-}$ level finds its equivalent within the Re d manifold. Figure 6 is the computed interaction diagram, with relevant blocks of $(Cp_3)^{3-}$ π levels at right, along with their symmetry representations. It is of course easy to derive the appearance and nodal properties of all $(Cp_3)^{3-}$ group MOs by constructing appropriate a and e representations from **12–14**, and together with the $Re_3O_6^{5+}$ fragment MOs of Figures 2–5, the resulting level scheme for $Cp_3Re_3O_6^{2+}$ in Figure 6 is straightforward.

Those MOs of the metal–oxygen core cluster that display π symmetry toward the faces of the Cp rings at the corners of the Re_3 triangle ($1a_2'$, $1e''$, $1a_2''$, $3e'$) interact strongly with the corresponding components of the HOMO block of six π MO linear combinations of the $(Cp_3)^{3-}$ system. The metal levels become strongly destabilized, as shown in Figure 6; the bonding (filled) levels resulting from these dominant interactions carry mainly Cp ligand character. The two $Re_3O_6^{5+}$ MOs of highest energy, $1a_1''$ and $2e''$, remain nearly unaffected because of their δ character toward the Cp rings and because of the even higher energy of the

(15) Only the pseudosymmetry of **1** and its unmethylated model with C_5H_5 rings is of course D_{3h}, but all MOs are practically unaffected by the lower "real" symmetries C_{3v} or C_{3h}, which are the most symmetric conformations possible.

(16) Group overlaps $\langle 1a_1'(Re_3O_6)/1a_1'(Cp_3)\rangle = 0.064$. $\langle 2a_1'(Re_3O_6)/1a_1'(Cp_3)\rangle = 0.076$. For comparison the group overlap $\langle 1a_2'(Re_3O_6)/1a_2'(Cp_3)\rangle = 0.265$.

Table I. Composition of the Six Valence Orbitals (EH) of $Cp_3Re_3O_6^{2+}$

MO	% Re_3	% Cp_3	% Re_3O_6	% O
2e′	66	10	90	24
$2a_1'$	43	8	92	49
1e′	38	33	67	29
$1a_1'$	27	43	57	30

empty, δ-symmetric π^* block of the arene ligand system. Of decisive importance are MOs $1a_1'$, 1e′, 2e′, and $2a_1'$ of the $Re_3O_6^{5+}$ unit; the ones we have depicted in Figures 3 and 5. MO $1a_1'$ of $Re_3O_6^{5+}$ can only interact with the in-phase a_1' orbital of the $(Cp_3)^{3-}$ moiety at lowest energy, shown in **15**.

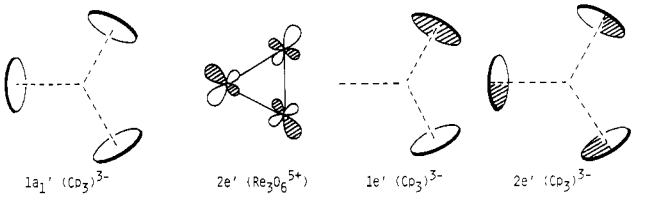

15 16

The metal-based $1a_1'$ level therefore remains at low energy, its Re–Cp (σ type) overlap is small and is equally small[15] for the $Re_3O_6^{5+}$ MO $2a_1'$ and **15**. Due to its δ symmetry and higher energy, $2a_1'$ interacts even less with **15** and stays put,[17] building the lowest empty level of the composite cluster. Also nearly unaffected is 1e′, because, as is apparent from Figures 2–5, the prevalent δ character of the Re contributions again prevents significant interaction with any of the filled Cp levels. 1e′ is in fact the highest occupied MO, housing two electrons. Still above the LUMO $2a_1'$ lies 2e′ of $Cp_3Re_3O_6^{2+}$; it originates from 2e′ of $Re_3O_6^{5+}$, which interacts with and is destabilized by Cp levels 1e′ and 2e′ as shown for one component (the one of Figure 3) in **16**.

So in summary the effect of three terminal Cp ligands upon the levels of $Re_3O_6^{5+}$ is to destabilize all low-lying ones except six "left-over" MOs. In ascending energetic order these are $1a_1'$, 1e′, $2a_1'$, and 2e′. We note that this is precisely the level sequence derived from the qualitative reasoning in the beginning. A low lying a_1' and e′ set of three levels carries four electrons—a triplet ground state is clearly expected from these model calculations. The lowest empty level is of a_1' type, about 1 eV above the e′ HOMO, and this will be relevant later. It is interesting to take a look at the orbital composition of the six valence levels of the cluster and this is done in Table I.

We note again some oxygen contribution to the wave functions but also quite an amount of Cp participation in the lower $1a_1'$ + 1e′ set. The whole cluster system displays metal to ligand covalent character but there is not much of direct metal–metal bonding. The computed Re–Re overlap populations of only +0.023 and the Re–O values of +0.447 reflect that the four electrons in $1a_1'$ and 1e′, corresponding to a Re–Re bond order of *formally* $^2/_3$, do not cause much direct Re–Re bonding. The cluster is held together and the Re–Re bond lengths are set mainly by Re–O bonding.

The extended Hückel results described so far of course may suffer from the method's inability to take into account electron repulsion and spin correlation. Given furthermore the aforementioned quantitative differences of Xα and EH results for $Re_3O_6^{5+}$, we also decided to perform a full Xα–SW calculation for the complete $Cp_3Re_3O_6^{2+}$ ion.

The pertinent part of the resulting Xα orbital energy spectrum is shown in Figure 7. A comparison with the corresponding part of the EH level spectrum in Figure 6 reveals a remarkable degree of similarity. As previously analyzed, four of the MOs localized on the core $Re_3O_6^{5+}$ remain at relative low energy, $1a_1'$, 1e′, $2a_1'$, and 2e′, containing four electrons, with the HOMO 1e′ being

(17) The group overlap of $2a_1'$ of Re_3O_6 (δ symmetry toward the Cp rings at each Re) with the appropriate empty group MO $2a_1'$ of the (Cp_3) fragment (a member of the highest energy block of π MOs shown in Figure 6) is only $\langle 2a_1'(Re_3O_6)/2a_1'(Cp_3)\rangle = 0.070$.

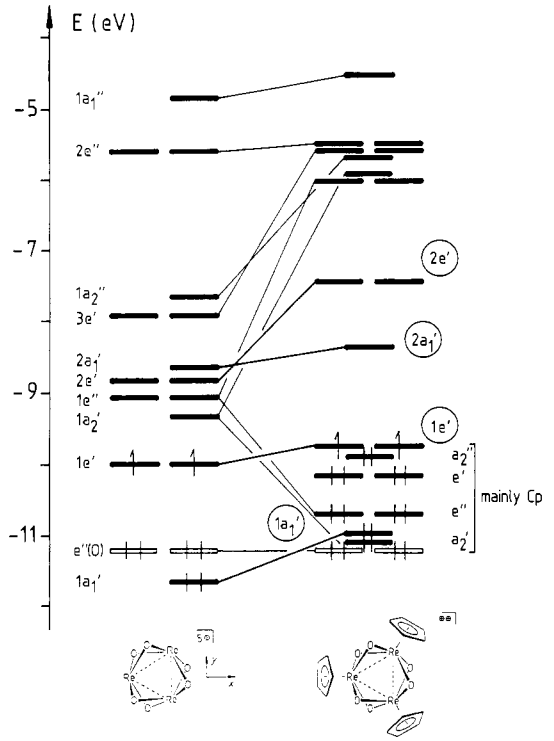

Figure 7. Xα–SW interaction diagram between the d-block levels of the $Re_3O_6^{5+}$ core and the MOs of the Cp_3^{3-} ligand system, with pseudo-D_{3h} symmetry. To facilitate the construction of this diagram, the levels of the $Re_3O_6^{5+}$ fragments are shifted uniformly, matching the topmost O 2p level e''(O) to that of the complete model cluster. Also shown are the orbitals constructed from the HOMO $e_1(\pi)$ of the three $C_5H_5^-$ ligands.

half-filled. In the energy region between the two occupied Re-based levels $1a_1'$ and 1e', we find six levels derived from the cyclopentadienyl e_1'' (π) MOs. They carry the bonding of the arene ligands to the metal atoms, thereby destabilizing their D_{3h} symmetry partners of the $Re_3O_6^{5+}$ core. An interaction diagram may be constructed as indicated in Figure 7 by aligning the Xα spectra for the $Re_3O_6^{5+}$ core and for the complete model cluster at the energy of the highest nonbonding, oxygen based-MO e''(O), which is of *pure* oxygen character in *both* cases. The conclusions of this analysis are identical with those derived from the EH fragment analysis. The spacings between various levels even turn out to be in satisfactory *quantitative* agreement. The HOMO–LUMO gap 1e' – $2a_1'$ is slightly larger in the Xα than in the EH MO spectrum (1.42 vs. 1.02 eV). The following energy difference, $2a_1'$ – 2e', which is of importance for analogous compounds to be discussed below, is almost equal (Xα, 0.92 eV; EH, 0.96 eV) as is also the energy spacing from the 2e' MO to the next higher level (Xα, 1.43 eV; EH, 1.35 eV). It is quite instructive (see Table II) to compare the composition of the relevant MOs of the core $Re_3O_6^{5+}$ and of the cluster ion $Cp_3Re_3O_6^{2+}$. A SW population analysis reveals that the low-lying levels $1a_1'$, 1e', 2e', and $2a_1'$ remain strongly localized on the Re atoms even in the full cluster ion with only very little contribution from the cyclopentadienyl ligands (maximum Cp_3 contribution: 11% in $1a_1'$). For the $1a_1'$ and 1e' MOs we notice differences to the Mulliken population results of the EH calculation, where sizable arene contributions had been found (see Table I). From the results of Table II one would expect that the Xα orbital contour plots for the low-lying $Re_3O_6^{5+}$ levels shown in Figure 5 should change only little in the complete cluster ion $Cp_3Re_3O_6^{2+}$; this is indeed the case, as may be seen in Figure 8.

The other levels, hardly affected by the interaction of the Re_3O_6 core with the three arene ligands, are the high-lying 2e'' and $1a_1''$ levels, which are strongly metal–oxygen antibonding (see also Figure 7). These MOs undergo almost no relative energy shifts. From the SW population analysis in Table II it becomes quite apparent that the Re_3O_6 core orbitals 1e'', $1a_2'$, $1a_2''$, and 3e' are destabilized in the assembled $Cp_3Re_3O_6^{2+}$ cluster ion because of

Table II. Composition of the Pertinent Xα–SW Valence Levels of the Core $Re_3O_6^{5+}$ and the Cluster Ion $Cp_3Re_3O_6^{2+}$

	$Re_3O_6^{5+}$		$Cp_3Re_3O_6^{2+}$		
MO	% Re_3	% O_6	% Re_3	% O_6	% Cp_3
$1a_1''$	56	44	50	43	7
2e''	58	42	54	38	8
3e'	65	35	54	16	30
$1a_2''$	59	41	53	20	27
$1a_2'$	87	13	52	7	41
1e''	72	28	48	12	40
2e'	81	19	71	22	7
$2a_1'$	65	35	62	35	3
1e'	72	28	59	32	9
$1a_1'$	77	23	79	10	11
Cp a_2''			16	27	57
Cp e'			34	20	46
Cp e''			29	27	44
Cp a_2'			42	8	50

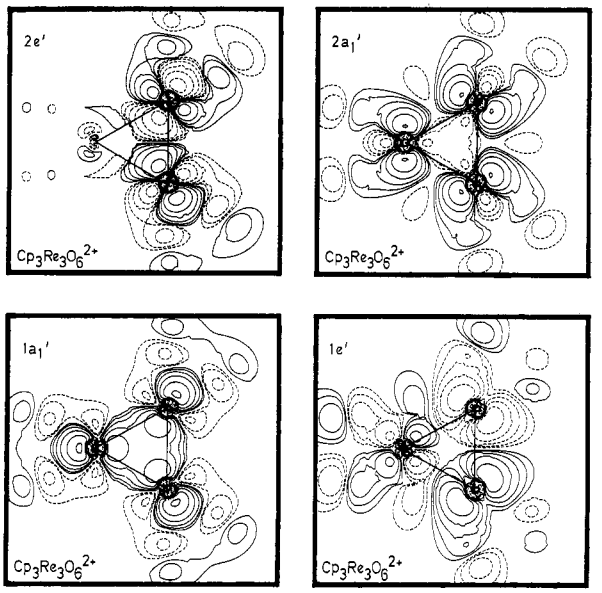

Figure 8. Xα–SW orbital contour plots for those levels of the ion $Cp_3Re_3O_6^{2+}$ corresponding to the MOs $1a_1'$, $2a_1'$, 1e', and 2e' of the core fragment $Re_3O_6^{5+}$ as shown in Figure 5. The same layout as in Figures 3 and 5 was used.

their strong interaction with their D_{3h} symmetry partners derived from the cyclopentadienyl π levels. For clarity, the corresponding bonding MOs (designated by Cp) are also shown in Table II. The metal as well as oxygen contribution to these levels is quite substantial as may be expected for a strong metal–arene interaction. From the results presented so far the evident conclusion is that in the ground state of the cluster ion $Cp_3Re_3O_6^{2+}$ two electrons should occupy a spatially degenerate pair of orbitals, 1e'. The cluster ion can therefore be viewed as a diradical.[18] One expects a triplet ground-state wave function that is spatially nondegenerate (of symmetry $^3A_2$, to be precise). Two further states of symmetry ^1E and $^1A_1$ should lie at higher energies due to their increased Coulomb repulsion. With the spin-polarized version of the Xα–SW method a triplet ground state was confirmed for the $Re_3O_6^{5+}$ core. From the results of this calculation the level spectrum for a similar treatment of the complete model cluster $Cp_3Re_3O_6^{2+}$ has been estimated (see Figure 9).

This procedure should result in an orbital spectrum rather close to that of a complete spin-polarized calculation since the pertinent level 1e' acquires only a very small contribution from the cyclopentadienyl orbitals. The block of the cyclopentadienyl orbitals of π descent remains completely filled. Also completely filled is

(18) Borden, W. T. In *Diradicals*; Borden, W. T., Ed.; Wiley: New York, 1982; Chapter 1.

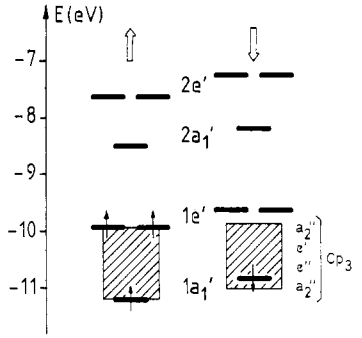

Figure 9. Pertinent part of a spin-polarized Xα–SW level scheme for the cluster ion $Cp_3Re_3O_6^{2+}$. Estimated by perturbation theory from the corresponding level spectrum of a non-spin-polarized calculation (see Figure 7) and a level splitting of 0.57 eV per 100% Re localization, as obtained from a self-consistent spin-polarized Xα–SW calculation of the $Re_3O_6^{5+}$ core. The filled set of Cp_3 (i.e. $e_1(\pi)$ derived) levels is indicated schematically for the sake of clarity.

now the 1e′(↑) level whereas its empty spin partner 1e′(↓) lies about 0.30 eV higher. So both methods, EH and Xα, lead to the prediction of two unpaired electrons in $Cp_3Re_3O_6^{2+}$, and this result should be valid for **1** with permethylated cyclopentadienyl groups as well. The reported observation of sharp lines in ^1H and ^{13}C NMR spectra of **1** seems to contradict a paramagnetic nature for **1** and indeed has been taken as an indication of the compound's diamagnetism.[1a] It should be mentioned, however, that there are other well-known examples of either triplet[19] or spin-crossover systems[20] in the literature where temperature-dependent sharp-line ^1H and ^{13}C NMR spectra are obtained. Three well-documented cases are shown in **17–19** and have been discussed in detail elsewhere.[20,21]

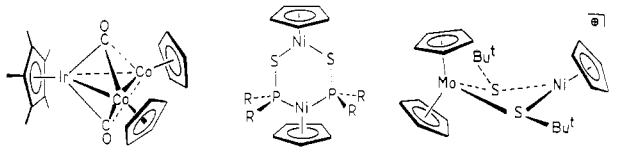

17 18 19

Obviously NMR spectra as a function of temperature, magnetic measurements and ESR work on **1** would be highly interesting. The level structures of Figure 6 and Figure 7 also suggest a well-developed electrochemistry of **1**. A one- or two-electron reduction should be possible, and the electrochemistry of **1** is presently under investigation.[22] Such studies seem to be of particular interest for **1**, because **1** represents a system (e.g. in contrast to **17–19**) where the unpaired electrons in the 1e′ level exhibit only a very minute delocalization of spin density onto the Cp ligands. The (numerically probably more realistic) $(Cp)_3$ contribution in Xα amounts to only 3% per Cp ring for our model $Cp_3Re_3O_6^{2+}$. For real **1** with methyl-substituted Cp rings, an ^1H NMR experiment of course applies only to protons even less influenced by direct spin delocalization and further away from the metal centers. It is an interesting question as to what extent

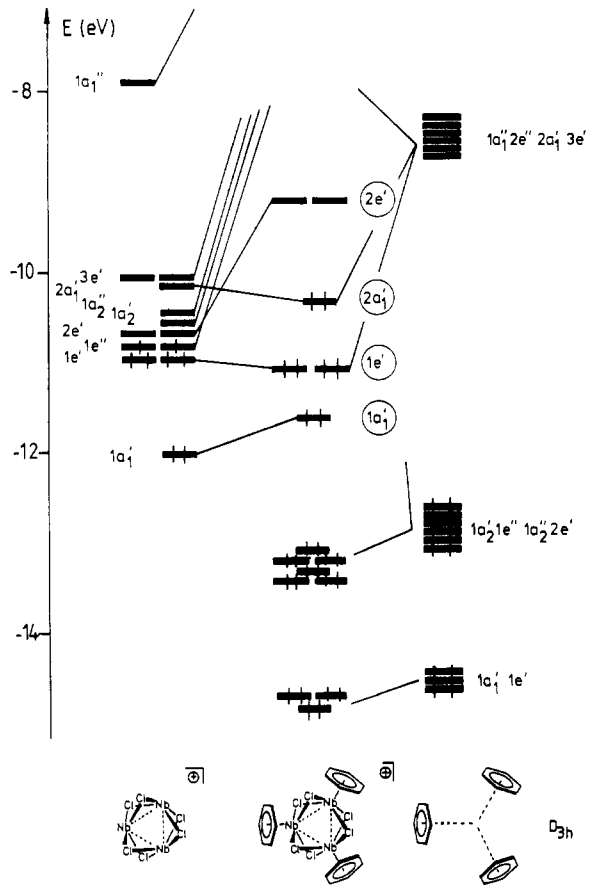

Figure 10. Interaction diagram (EH) between the d-block levels of the $Nb_3Cl_6^+$ core and the MOs of the $(C_6H_6)_3$ ligand system, with D_{3h} symmetry and benzene σ levels omitted. The highest $Nb_3Cl_6^+$ level, 2e″, is outside the energy scale of the diagram.

two unpaired electrons, if present in the 1e′ level of the cluster, will show up in ^1H or ^{13}C nuclear magnetic resonance experiments.

If, on the other hand, experiments should prove **1** to be indeed diamagnetic or, in other words, if qualitative symmetry-based reasoning, extended Hückel calculations, and Xα calculations all lead to an identical but incorrect description of the electronic structure of **1**, then an even more challenging case is at hand, telling us that either our modeling of pentamethylcyclopentadienyl by Cp leads to unexpected level inversions that have to be understood or even indicating some basic pathological failing at the level of theories applied here. In any case, the triplet or singlet state of **1**, if experimentally verified in an unequivocal manner, will teach us an important lesson.

Related Systems

Changing the occupation pattern of the block of six valence levels of **1** leads us directly to the halogeno bridged trimetal cluster species **5–9** already mentioned in the beginning. The monocations $Bz^*_3M_3Cl_6^{n+}$ (Bz^* = η^6-hexamethylbenzene) with M = Ta and Nb, structurally characterized for M = Nb and X = Cl, are diamagnetic and in our level scheme of **1** would correspond to four electrons more than in the latter. 1e′ and $2a_1'$ would be filled. When we perform an EH model calculation for $(C_6H_6)_3Nb_3Cl_6^+$ (D_{3h}), a level diagram in terms of interacting fragments $Nb_3Cl_6^+$ and $(C_6H_6)_3$ results as shown in Figure 10. At left the $Nb_3Cl_6^+$ levels are at higher energy relative to the previous $Re_3O_6^{5+}$ case, and 11 levels (1e′–3e′) appear within a narrow energy range of 1 eV. The $(C_6H_6)_3$ subsystem at right has its MOs of the HOMO and LUMO block at lower energy than the $(Cp_3)^{3-}$ ligand set. The resulting overall picture is identical, however, with that of the Re system: again a set of six levels, $1a_1'$–2e′, destabilized the least by the arene groups, holds the valence electrons, now a total of 8; $2a_1'$ is the HOMO. The orbitals are of the same type as for **1**, but a difference lies in their composition, which reveals much

(19) Hermann, W. A.; Barnes, C. E.; Zahn, T.; Ziegler, M. L. *Organometallics* **1985**, *4*, 172–180.
(20) Kläui, W.; Schmidt, K.; Bockmann, A.; Hofmann, P.; Schmidt, H. R. *J. Organomet. Chem.* **1985**, *286*, 407–418.
(21) For a discussion of **17** and of related systems, see: Pinhas, A. R.; Albright, T. A.; Hofmann, P.; Hoffmann, R. *Helv. Chim. Acta* **1980**, *63*, 29–49. Compound **18** has been discussed in ref 19 and compound **19** by Werner et al. (Werner, H.; Ulrich, B.; Schubert, U.; Hofmann, P.; Zimmer-Gasser, B. *J. Organomet. Chem.* **1985**, *297*, 27–42), with respect to their electronic structures.
(22) Herrmann, W. A. private communication. The ease of reduction may of course also depend upon other factors, like the shielding of the Re_3O_6 core by the three negatively charged surrounding pentamethylcyclopentadienyl rings, which may hamper electron transfer or which may even lose electrons easily themselves, leading to oxidation processes within the arene ligand system.

Table III. Parameters Used in the Extended Hückel Calculations

orbital		H_{ii}, eV	ζ_1	ζ_2	C_1[a]	C_2[a]
Re	6s	−10.54	2.398			
	6p	−6.68	2.372			
	5d	−14.88	5.343	2.277	0.6377	0.5657
Nb	5s	−9.19	1.890			
	5p	−5.85	1.850			
	4d	−11.37	4.08	1.64	0.6401	0.5516
O	2s	−32.30	2.275			
	2p	−14.80	2.275			
Cl	3s	−30.0	2.033			
	3p	−15.0	2.033			
C	2s	−21.40	1.625			
	2p	−11.40	1.625			
H	1s	−13.60	1.3			

[a] Two Slater exponents for the double-ζ d functions, C_1 and C_2, are the contraction coefficients.

more metal character and less Cl or C_6H_6 contributions to the wave functions (92, 75, 63, and 87% Nb contribution to levels $1a_1'$, $1e'$, $2a_1'$, and $2e'$). Less ligand–metal covalency, in accord with intuitive expectations, is found here, the occupancy of $1a_1'$–$2a_1'$ with eight electrons yields a Nb–Nb overlap population of 0.087, the Nb–Cl value being 0.382. Again no strong metal–metal bonds are indicated, the additional four electrons (compared to **1**) enter MOs of more or less metal–metal nonbonding character (see the plots given above). The larger dimensions of the Nb cluster are a consequence of the longer, less covalent Nb–Cl bonds, which are pure σ bonds in contrast to the Re–O bonds with some double-bond character due to stronger p–d bonding from oxygen 2p atomic orbitals to Re functions.

The electronic level scheme (Figure 10) for $(C_6H_6)_3Nb_3Cl_6^+$ is consistent with the fact, that experimentally the permethylated derivative **5** can be oxidized[9] to the corresponding dication, **6**, which has been isolated as its $TCNQ^{2-}$ salt. ESR spectroscopy and magnetic measurements have shown that one unpaired electron is present in this radical system and that it resides on the niobium atoms. From Figure 10 it is also seen that oxidation will remove one electron from the highest occupied level $2a_1'$, which is essentially nonbonding or at best very weakly Nb–Nb bonding. The resulting doublet ground state of the oxidized cluster dication **6** (seven electrons in the relevant M_3 levels) then will have its remaining single electron in $2a_1'$. No electronically induced geometric deviation from threefold symmetry upon oxidation is expected, and no significant Nb–Nb bond length changes should occur, as a largely nonbonding electron is lost. Indeed the single-crystal X-ray diffraction study of Eisenberg, Miller, et al.[9] shows that the Nb–Nb distance in **6** is 3.335 (9) Å as compared to 3.334 (6) Å in **5** and that no significant distortion, comparable to other cases of M_3 clusters with Jahn–Teller instabilities,[23] is found.[24] It is furthermore interesting to note that in contrast to the well-characterized oxidation chemistry of this class of trinuclear $(C_6Me_6)_3M_3X_6^+$ clusters (M = Nb, Ta; X = Cl, Br) their reduction (electrochemically or chemically) results in irreversible decomposition. The niobium/chloro system, for instance, is irreversibly destroyed at potentials below 1.8 V in electrochemical experiments.[7] This is again consistent with Figure 10: additional electrons are bound to enter the $2e'$ orbital set, which is already appreciably metal–arene antibonding as well as metal–metal antibonding. Additionally, a recent electrochemical study[9b] shows that $(C_6Me_6)_3Nb_3Cl_6^+$ can be reversibly oxidized not only to the dication but also to the +3 and +4 charged species in solution. The tetracation has the same electron count as Fischer's Zr and Ti systems with a +1 charge.

(23) One such case, analyzed in detail in ref 3, is $Mo_3S_2Cl_9^{3-}$: Huang, J.; Shang, M.; Liu, S.; Lu, J. *Sci. Sin. (Engl. Transl.)* **1982**, *25*, 1270. Here an e'' orbital is half-filled.

(24) The extremely small difference between the two observed independent Nb–Nb distances in **6** probably is a consequence of the crystallographically imposed mirror symmetry of the $TCNQ^{2-}$ salt in the solid state.

(25) Basch, H.; Viste, A.; Gray, H. B. *Theor. Chim. Acta* **1965**, *3*, 458–464.

Table IV. Muffin-Tin Radii r and Exchange Parameters α Used in the SCF Xα–SW Calculations

region	r, Å	α
Re	1.249	0.693
O	0.917	0.744
C	0.882	0.759
H	0.491	0.777
outer sphere	2.835;[a] 4.665[b]	0.727[c]

[a] $Re_3O_6^{5+}$. [b] $Cp_3Re_3O_6^{2+}$. [c] The same value has been used in the intersphere region.

Finally, without explicit calculations we refer to the last group of such trimetal clusters with group 4 metals, prepared by Fischer and Röhrscheid, namely to **9** (M = Ti, Zr). These cations contain one valence electron more than Herrmann's Re compound and have been reported to display magnetic behavior in agreement with the presence of one unpaired electron.[6] The degenerate $1e'$ level pair of Figure 10 houses three electrons in these cluster ions, and we should expect a dynamic or static Jahn–Teller distortion in their ground state. It seems quite challenging to take a look at the solid-state structures and at the electrochemistry for these cases too. This would be of particular interest here, because the molecular structure of a dication $(C_6Me_6)_3Zr_3Cl_6^{2+}$ has been recently determined by X-ray methods.[6b] No information about its magnetism is available, however. Naturally this study also leads one to think about the possible existence of hitherto unknown relatives of either **1** or of the hexamethylbenzene systems. Adjusting the valence electron count between four and eight (i.e. between a half-filled $1e'$ and a fully filled $2a_1'$ level) allows various ionic or neutral, diamagnetic, or paramagnetic species with $C_5Me_5^-$ or C_6Me_6 type ligands and bridging X groups ($X = O^{2-}$, halogen$^-$, S^{2-}, SR^-, OR^- etc.) to be assembled and we can leave this to the interested reader. In any case, certainly more fascinating chemistry is to be expected in this field.

Conclusions

Both extended Hückel and SCF Xα–SW calculations have been used to describe bonding and structure of the recently synthesized cluster ion $[(\eta^5\text{-}C_5Me_5)_3Re_3(\mu\text{-}O)_6]^{2+}$ (**1**). In agreement with simple qualitative MO arguments both independent electronic structure computation methods give the same consistent picture. **1** should possess two unpaired electrons leading to paramagnetism and a triplet ground state. The nature and ordering of the relevant valence orbitals for **1** and for a series of related M_3 clusters of the U_6 type has been described in detail and allows an understanding of the known chemistry of such compounds and an extrapolation to hitherto unknown systems. Although the basic conclusions for **1** and its congeners are mainly symmetry and overlap determined, the agreement of EH and SCF Xα–SW calculations with respect to the relative MO energy orderings and to the calculated wave functions is remarkable. The results presented here challenge further experimental investigations for **1** in order to unequivocally assess its triplet or singlet nature. Should a closed-shell ground state be firmly established for **1**, contrasting the theoretical results, then some of our basic concepts of cluster bonding for such species may have to be revisited.

Acknowledgment. The authors are grateful to Profs. R. Hoffmann and W. A. Herrmann for communicating results prior to publication and for valuable discussions and comments. We thank P. Stauffert for running some of the EH calculations. The generous support from the Fonds der Chemischen Industrie and the cooperation of the staff of the Leibniz Rechenzentrum, München, FRG, is also gratefully acknowledged. This work has been partially supported by the Deutsche Forschungsgemeinschaft.

Appendix

The extended Hückel calculations[11] were performed for the two model systems $(C_5H_5)_3Re_3O_6^{2+}$ and $(C_6H_6)_3Nb_3Cl_6^+$; i.e., we replaced the permethylated arene ligands by their parent systems. The geometries used were adapted from the reported X-ray structure data of the literature[1,8] and idealized. For the Re_3 system the C_5H_5 rings were oriented in such a way as to create overall

C_{3v} symmetry. The $Re_3O_6^{5+}$ core had exact D_{3h} geometry, and the symmetry labels of this point group have been used throughout also for the cluster, because the symmetry perturbation due to the C_5H_5 rings is minute. The geometric parameters used are as follows: Re–Re = 275 pm, Re–O = 194.5 pm, Re–C = 225 pm, C–C = 140 pm, C–H = 108 pm; C_5H_5, local D_{5h} symmetry; angles between the Re_3 plane and the Re_2O planes = 123°. For the Nb_3 cluster cation exact D_{3h} symmetry was used with the three benzenes oriented "upright", i.e. with three carbons above and three below the Nb_3 plane. The following parameters were used: Nb–Nb = 333.5 pm, Nb–C = 240 pm, C–C = 149 pm, C–H = 108 pm, Nb–Cl = 249 pm; C_6H_6, D_{6h}; angles between the Nb_3 plane and the Nb_2Cl planes = 123°. For both cluster cations a charge-iterative calculation was performed to obtain self-consistent (SCCC) valence state ionization potentials (H_{ii} values) for the Re and Nb atoms. *A*, *B*, and *C* parameters in the SCCC calculations are from ref 26. A modified Wolfsberg–Helmholz formula[27] was used throughout. The atomic parameters used for the metals (converged H_{ii} values and wave functions[28]) and for C, H, O, and Cl are given in Table III.

The same geometries as described above were used in our SCF Xα–SW calculations on the fragment $Re_3O_6^{5+}$ and the model cluster cation $Cp_3Re_3O_6^{2+}$. An overlapping sphere parametrization was chosen to obtain a more realistic muffin-tin description of the electronic potential, especially in the complete cluster including the cyclopentadienyl ligands. The muffin-tin sphere radii for Re and O were determined by applying Norman's criterion[29] to the $Re_3O_6^{5+}$ core, with a scaling factor of 0.85 used. The radii for C and H were taken from a previous Xα–SW calculation on ferrocene.[30] The maximum values in the partial wave expansions included in the calculations were $l = 2$ for Re, $l = 1$ for O and C, $l = 0$ for H, and $l = 4$ in the extramolecular region. The atomic exchange parameters for Re and O were taken from the tables provided by Schwarz;[31] those for C and H were chosen as in a previous calculation.[30] A weighted average of the atomic values was employed in the intersphere and in the extramolecular region. The various parameters used in the Xα–SW calculations are collected in Table IV.

A quasirelativistic[32] version of the Xα–SW method has been used that has proven well suited for large molecules containing heavy elements.[33] The core charge densities for C ([He]), O ([He]) and Re ([Xe]$4f^{14}$) were kept fixed as obtained from atomic Xα calculations (of relativistic type for Re). All other electrons were considered fully in the iterations toward self-consistency, but spin–orbit interaction and spin polarization were neglected. To mimic the electrostatic contributions of the surrounding ions to the electronic potential a charge to compensate that of the cluster was distributed uniformly over the outer sphere (Watson sphere[12b]). In the case of $Re_3O_6^{5+}$, the effect of this charge included, at least approximately, the destabilizing electrostatic interaction of the three $C_5H_5^-$ anions on the levels of the core fragment.

For the $Re_3O_6^{5+}$ a self-consistent spin-polarized Xα–SW calculation has also been carried out to estimate the splitting between corresponding levels of the majority spin and minority spin potentials. For the d-block levels this splitting was roughly proportional (±5%) to the localization of the various orbitals inside the Re spheres. The average value was calculated as 0.57 eV per 100% Re localization. This value was then used to estimate the effect of spin polarization on the level structure of the full cluster $Cp_3Re_3O_6^{2+}$. Thereby each level of the non-spin-polarized calculation was split proportionally to its Re contribution, lowering the majority spin level and raising the minority spin level by equal amounts (see Figure 9).

In a SW population analysis the charge fraction localized in the intersphere and in the extramolecular region cannot be unambiguously assigned to the various atoms. All SW orbital populations quoted have been obtained by allocating this charge to the atoms in proportion to the orbital charge fraction already localized inside the corresponding sphere.[34] Results of this scheme should be interpreted with due caution and, by their derivation, cannot be directly compared to Mulliken charges routinely derived in EH calculations. However, valuable although only qualitative insight may be obtained from such a SW population analysis.[34]

(26) Munita, R.; Letelier, J. R. *Theor. Chim. Acta.* **1981**, *58*, 167–171.
(27) (a) Ammeter, J. H.; Bürgi, H.-B.; Thibeault, J. C.; Hoffmann, R. *J. Am. Chem. Soc.* **1978**, *100*, 3686–3692. (b) Hoffmann, R.; Hofmann, P. *J. Am. Chem. Soc.* **1978**, *98*, 598–604.
(28) Re: Shaik, S.; Hoffmann, R.; Fisel, C. R.; Summerville, R. H. *J. Am. Chem. Soc.* **1980**, *102*, 4555–4572. Nb: Summerville, R. H.; Hoffmann, R. *J. Am. Chem. Soc.* **1976**, *98*, 7240–7254.
(29) Norman, J. G. *Mol. Phys.* **1976**, *31*, 1191–1198.
(30) Rösch, N.; Johnson, K. H. *Chem. Phys. Lett.* **1974**, *24*, 179–184.
(31) Schwarz, K. *Phys. Rev. B* **1972**, *85*, 2466–2468; *Theor. Chim. Acta* **1974**, *34*, 225–231.
(32) Thornton, G.; Rösch, N.; Edelstein, N. *Inorg. Chem.* **1980**, *19*, 1304–1307. Heera, V.; Seifert, G.; Ziesche, P. *J. Phys. B*: **1984**, *17*, 519–530.
(33) Rösch, N.; Streitwieser, A., Jr. *J. Am. Chem. Soc.* **1983**, *105*, 7237–7240. Rösch, N. *Inorg. Chim. Acta* **1984**, *94*, 297–299. Andersen, R. A.; Boncella, J. M.; Burns, C. J.; Green, J. C.; Hohl, D.; Rösch, N. *J. Chem. Soc., Chem. Commun.* **1986**, 405–406. Hohl, D.; Rösch, N. *Inorg. Chem.* **1986**, *25*, 2711–2718.
(34) Schichl, A.; Rösch, N. *Surf. Sci.* **1984**, *137*, 261–279.